



Open Access : : ISSN 1847-9286

www.jESE-online.org

Original scientific paper

Electrodeposition of polyfunctional Ni coatings from deep eutectic solvent based on choline chloride and lactic acid

Dmytro Uschapovskiy, Viktoria Vorobyova, Georgii Vasyliiev✉ and Olga Linucheva
National Technical University of Ukraine "Igor Sikorsky Kyiv Polytechnic Institute", 37, Prospect Peremohy, Kyiv-56, 03056, Ukraine

Corresponding author: ✉ g.vasyliiev@kpi.ua; Tel.: +38-096-924-9888; Fax: +38-044-204-9773

Received: June 8, 2022; Accepted: September 9, 2022; Published: September 13, 2022

Abstract

The process of electrodeposition of nickel coatings from electrolytes based on a deep eutectic solvent (DES) mixture of choline chloride and lactic acid with a molar ratio of 1:3 was studied. The physicochemical properties and characteristics of DES, namely, conductivity, FT-IR and NMR analysis were determined. FT-IR results confirmed that H-bonds occurring between two components in DES were the main force leading to the eutectic formation. Electrochemical techniques were used to characterize the deposition process and scanning electron microscopy was used to study the deposit morphology. Based on polarization measurements, it has been found that at $\text{NiCl}_2 \cdot 6\text{H}_2\text{O}$ content of 1.14 M and a temperature of 75 °C, the limiting current density of nickel electrodeposition was near 2 A dm^{-2} . The polarization of the cathodic nickel deposition varied within -0.63 to 1.1 V at current density of 0.25 A dm^{-2} . It has been shown that an increase of water content in the electrolyte does not significantly affect the current efficiency of the nickel electrodeposition process, which was in a range 85-93 %. However, the increase in water content contributes to the increase of heterogeneity and crystal grains size distribution of galvanic deposits. The established values of the Wagner number indicate the predominance of the primary current density distribution in the process of electrodeposition of nickel coatings. Galvanic coatings possess a highly developed nanostructured surface, exhibit increased capillary properties, and can be used as electrode materials for the process of electrolysis of water.

Keywords

Ni plating; current efficiency; polarization; crystal grains size; nanostructured surface

Introduction

One of the modern directions of electroplating is the electrodeposition of coatings from non-aqueous electrolytes, in particular, based on deep eutectic solutions - mixtures of organic compounds - the so-called DES [1-5]. The DES formation process is coupled with the formation of

donor-acceptor bonds [6], and the melting point of the selected eutectic mixture is lower than the individual components. DES-s are similar in their properties to ionic liquids, which makes promising their application in such areas of technical electrochemistry as electroplating [7-9] or chemical current sources [10-12]. Electrolytes based on DES are widely used for electrodeposition of metals, the main component-donor (HBD) of which is choline chloride. The following organic compounds can be acceptors (HBA): organic acids, polyhydric alcohols, urea and its derivatives. A significant amount of printed works has been devoted to the electrodeposition of metal coatings from electrolytes based on DES, such as ethaline (a mixture of choline chloride and ethylene glycol) [7,9,13-15] and reline (a mixture of choline chloride and urea) [16-18]. It is well known that galvanic nickel coatings, in terms of their physical, mechanical, and electrochemical properties, are multifunctional and are used both in the fields of special surface treatment of parts and of electrochemical energy conversion. In-depth investigation of nickel coatings' electrodeposition process from electrolytes based on DES can expand their range of properties and applications.

Ethaline and reline are most often used as the basis of the electrolyte in the electrodeposition of nickel coatings, as evidenced by the data of most known works [7,9,13-18]. In particular, the disadvantages of the corresponding DES include the following. Although the operating temperature of the nickel electrodeposition process from ethaline-based solutions is 70 °C, the component (donor) of this solution is highly toxic ethylene glycol. The main disadvantage of reline-based electrolytes is the high operating temperature (90–100 °C), and hence the increased energy consumption of the process. Thus, the urgent scientific task is to select a donor for the solvent of the nickel-plating electrolyte based on choline-containing DES, which would meet the environmental safety conditions and cost-effectiveness of the nickel-plating process. A deep eutectic mixture based on choline chloride and lactic acid (LC) is of considerable interest [19-21]. These compounds were chosen because they can be obtained from natural sources, used as food additives, and generally recognized as safe (GRAS) [22,23]. The studies have shown that the molar ratio of choline chloride and lactic acid can vary from 1:1 to 1:3 without considerable reduction of HBA:HBD interaction [24]. That is, the mass fraction of the cheaper and environmentally friendly component (donor) – lactic acid, is greater than for ethylene glycol in ethaline. Electrodeposition of zinc from LC mixture formed by choline chloride - lactic acid (1:2) was studied [20]. The deposition process was conducted in a two-electrode cell. The low-carbon steel was used as the cathode and the zinc plate as the anode. The deposition of Zn was carried out using a constant current mode. Cyclic voltammetry results showed that the electrochemical stability window of LC is approximately 2.3 V. The onset of Zn reduction (vs. Ag/AgCl) in LC occurs at $E = -1.4$ V and there is a clear current cross-over loop during the reduction process. The SEM study showed that the morphology of the coatings evolves into domains of co-aligned platelets with a fast growth direction roughly perpendicular to the interface.

This work is devoted to the investigation of the nickel coating electrodeposition process from the electrolyte based on a deep eutectic mixture of choline chloride and lactic acid with a molar ratio 1:3 and the investigation of the deposited Ni coating properties as a promising electrode material for electrolysis of water.

Experimental

Choline chloride 99 % and lactic acid 90 % (Acros Organics), nickel chloride and potassium chloride (Khimlaborreaktiv) of reagent grade were used. The DES was prepared by the heating method. Briefly, choline chloride and lactic acid were mixed in sealed 100 mL glass flasks in molar

ratios. The mixtures were placed in a round-bottom flask and continuously stirred at 60 °C, 300 rpm in a magnetic stirrer until the mixture formed a clear solution. A DES is often made with a mixture of salt and a hydrogen bond donor molecule which can form bonds with the halide in the salt, as shown in Figure 1.

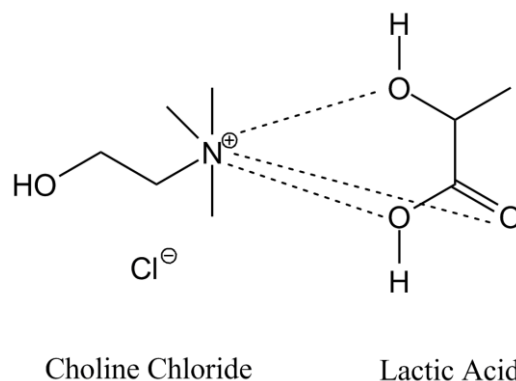


Figure 1. Hydrogen bond donor (HBD) and acceptor (HBA) studied in this work lead to the formation of (hydrogen bond between) choline chloride and lactic acid

The synthesis of DES was confirmed by the nuclear magnetic resonance (NMR) spectrometry method (Bruker Ascend 300). A nuclear magnetic resonance (NMR) spectrometer operating at 300 MHz was used to record the ^1H NMR spectra of the DES. All samples were dissolved in D_2O . The chemical shift corresponding to the methyl group peak has been used as a reference.

Fourier transformed infrared (FT-IR) spectra of the DESs were obtained using a Bruker Tensor 27 (Bruker Corp, Massachusetts, USA). A total of 14 scans were measured at 4 cm^{-1} resolution with a scan rate of 22 scans min^{-1} . Measurements were done between 650 and 4000 cm^{-1} using air as a reference.

The DES for nickel plating electrolyte was prepared by fusing choline chloride with lactic acid in a molar ratio 1:3 at $70\text{ }^\circ\text{C}$. After homogenization of the system, $\text{NiCl}_2\cdot 6\text{H}_2\text{O}$ was dissolved in the obtained DES to give a concentration of 1.14 M ($\text{H}_2\text{O}/\text{Ni}$ molar ratio = 6). Additionally, distilled water was added to the electrolyte in $\text{H}_2\text{O}/\text{Ni}$ molar ratio = 12 and 18.

To determine the width of the electrochemical window the cycling voltammetry technique was used. The electrochemical window determines the range of potentials where the electrolyte is neither oxidized nor reduced. Traditional three-electrode electrochemical cell was used with a saturated silver chloride reference electrode ($E = +0.2\text{ V vs. NHE}$) (SSCE). A saturated silver chloride reference electrode was connected to the cell *via* an intermediate beaker and a salt bridge filled with saturated KCl solution to prevent any mixing of solutions. The pair of platinum electrodes were polarized with direct current in the potential range -1.2 to $+1.2\text{ V vs. SSCE}$. The scanning rate was 50 mV s^{-1} . The scan was performed 3 times to assure data convergence.

The cathodic potentiodynamic curves in the investigated Ni-electrolyte were obtained on a working nickel electrode (99.98 %) of cylindrical shape, pressed into Teflon. The surface of the working electrode was 0.5 cm^2 . Before obtaining the curves, the working surface of the electrode was mechanically degreased with potassium carbonate and, after rinsing in distilled water, etched in 10 % HCl solution. Nickel plate of electrodeposited nickel (99.98 %) was used as an auxiliary electrode. As a reference electrode, a silver wire (95.9 %) was used, which was placed directly in the cell. The potential of silver wire was measured vs. SSCE electrode in the DES solution and was found to be $+0.1\text{ V vs. SSCE}$. Polarization curves were obtained in a standard three-electrode cell. The potential values are given versus the potential of the silver wire. The scan rate was 10 mV s^{-1} . The

temperature was 75 ± 3 °C. The polarization of the cathodic nickel deposition process (ΔE) was determined at the current density of 0.25 A dm^{-2} .

The cathodic potentiodynamic curves of electrochemical evolution of hydrogen on electrodeposited nickel coatings were obtained in 0.1 M KOH. A saturated silver chloride reference electrode was connected to the cell *via* two intermediate beakers and a Luggin capillary. A platinum metal plate with an area of 0.53 cm^2 was used as a counter electrode. The potential scan rate was 10 mV s^{-1} . The temperature was 20 °C.

The Ametek VersaStat 3-200 digital potentiostat with VersaStudio 12 software was used to perform polarization measurements, as well as to measure the electrical conductivity of the investigated solutions. The resistance of the electrolyte was measured in a standard cell with two platinum electrodes, the area of each was 2 cm^2 , the interelectrode distance was 0.5 cm, the frequency of alternating current was 10^3 to 10^6 Hz. The electrical conductivity of the electrolyte was calculated based on the values of the resistance of the electrolyte and the cell constant was determined using 0.01 M KCl.

Electrodeposition of nickel coatings was performed on rectangular steel samples of steel 08kp (European analogue Fe37-3FN) with an area of 6 cm^2 . Electrodeposition of nickel coatings was performed from an electrolyte prepared based on the investigated DES. Also, to compare the properties of the coatings obtained from the electrolyte based on DES, matte and bright nickel coatings were tested, which were electrodeposited from the Watts bath. For electrodeposition of bright coatings in the Watts bath the saccharin at a concentration of 0.5 g dm^{-3} was added. Operating current densities ranging from 0.5 to 2 A dm^{-2} . Electrodeposition was performed in a cylindrical glass cell with a cylindrical nickel anode made of nickel foil (99.98 %) $200 \mu\text{m}$ thick. The electrolyte temperature was 75 ± 3 °C. The current efficiency of the nickel electrodeposition process was determined based on the gravimetric method using analytical balance RAWAG AS 220 R2. As a dc source, a rectifier B5-43 was used. The thickness of the electrodeposited coatings was 5 to $20 \mu\text{m}$.

The investigations of capillary uplift of liquids on the surface of nickel coatings were performed by immersing samples with nickel coatings in a Petri cup with ethyl alcohol (98 %) and distilled water. Rectangular steel samples with electrodeposited nickel coatings were placed at an angle of 90° to the test liquid mirror. The depth of immersion of the sample edge was 3 mm. The height of the liquid uplift on the surface of the sample was measured and recorded 15 min after the start of exposure with an accuracy of 0.5 mm.

SEM-studies of the surface of electrodeposited nickel coatings were performed using TESCAN VEGA3 microscopes equipped with an EDX analyzer Bruker Quantax EDS and PEM106-I equipped with an Oxford HKL Channel-5 EDX analyzer.

Results and discussion

Characterization of deep eutectic solvents and DES-based electrolyte

From the FT-IR spectrum in Figure 2, several bands characteristic groups of DES scan are seen. The large band at 3432.9 cm^{-1} could be assigned to O-H group. The bands appearing at 2920.7 and 2849.1 cm^{-1} correspond to C-H stretching vibration. The frequency at 3221 cm^{-1} is assigned to the O-H stretching frequency associated with OH-Cl of choline chloride. The OH stretching region of lactic acid contains broad overlapping bands centered on 3420 cm^{-1} that is typical of carboxylic acid, forming strongly bonded dimer rings through intermolecular H-bonding between C-O and O-H groups. The outline of the bond may be due to the combined bonding of choline chloride and lactic

acid molecules overlapping in the O-H and N-H bond. Two weak peaks were observed at 2987 cm^{-1} in DES, indicating C-H stretching bonds, but shifted to a slightly lower wave number.

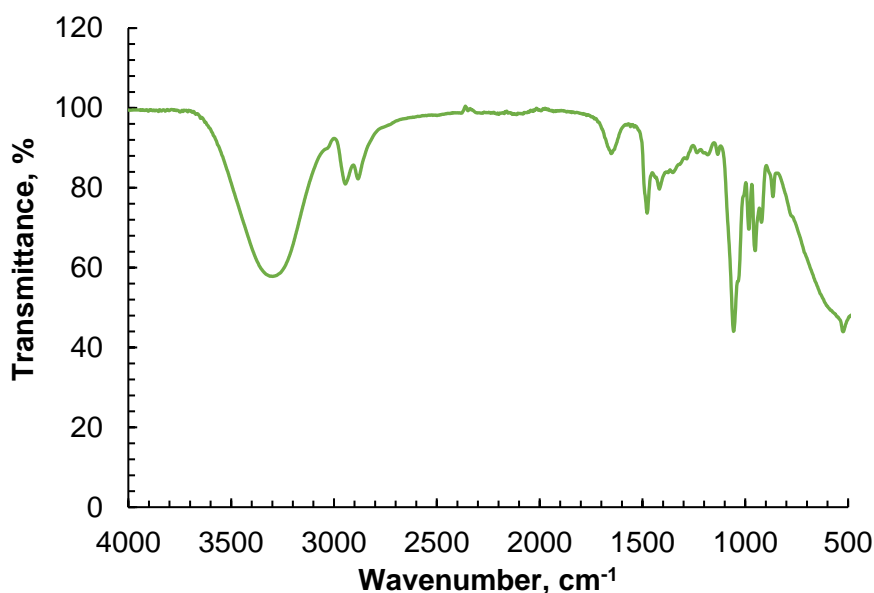


Figure 2. FT-IR spectrum of choline chloride – lactic acid

The ^1H NMR analysis has been used to study the ionization states of protons and determine the structure of the molecules (Figure 3). The ^1H NMR analysis on the synthesized choline chloride – lactic acid DES was performed. The chemical shift for choline chloride appeared at $\delta = 4.95\text{ ppm}$. The peak of lactic acid at 1.48 ppm has an integral value of 2.11, while at 3.44 ppm , labeled with number 9, the peak of choline chloride – lactic acid has an integral value of 2.00. Thus, the molar ratio of the choline chloride – lactic acid is indeed 1:3. These findings explain that the OH groups of lactic acid may interact with choline chloride and then form intermolecular hydrogen bonds, which enhance the solvation capacity of DES.

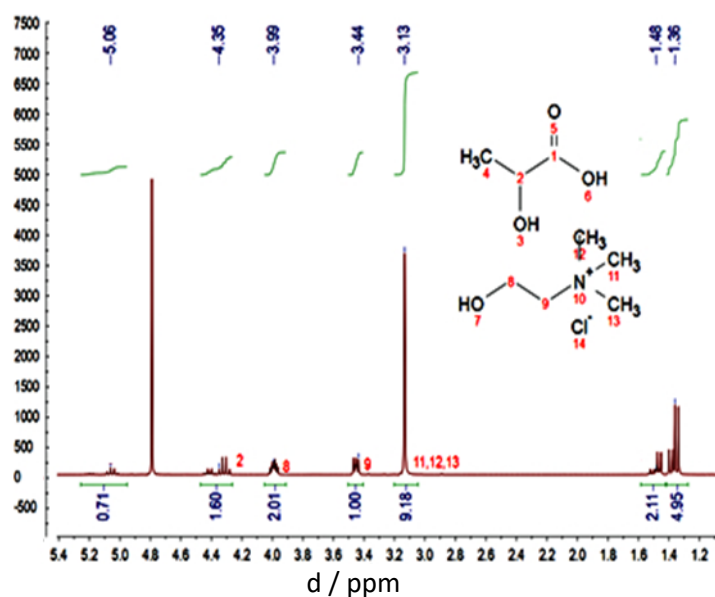


Figure 3. ^1H NMR spectrum of the DES choline chloride – lactic acid

Figure 4 presents a typical cyclic voltammogram for DES, which shows an electrochemical stability window (ESW) on Pt electrodes from about -0.3 to $+1.0\text{ V}$ (electrode potential vs. SSCE). Pure solvents show the widest stability window, *e.g.*, choline chloride-lactic acid ESW exceeds 1.33 V .

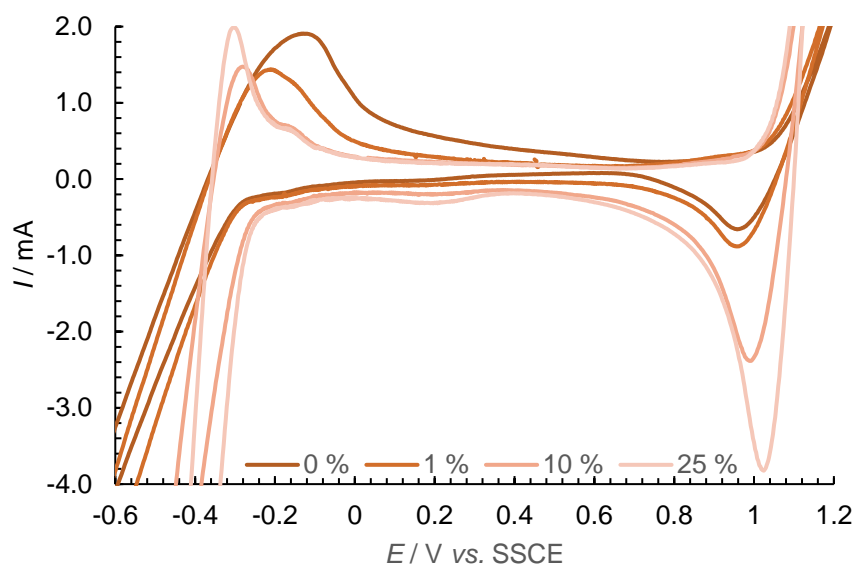


Figure 4. Cyclic voltammograms of choline chloride – lactic acid with various concentrations of water (0-25 %)

Investigation of nickel electrodeposition process

According to [25], the addition of water to the nickel-plating electrolyte based on ethaline has a positive effect on the morphology of deposited metal. The effect of water content that corresponds to molar ratio H_2O/Ni [M/M] = 12 and 18 is especially noticeable. Therefore, the effect of a similar amount of water was investigated in the electrolyte based on choline chloride and lactic acid. The polarization curves obtained in the investigated nickel-plating electrolyte are shown in Figure 5.

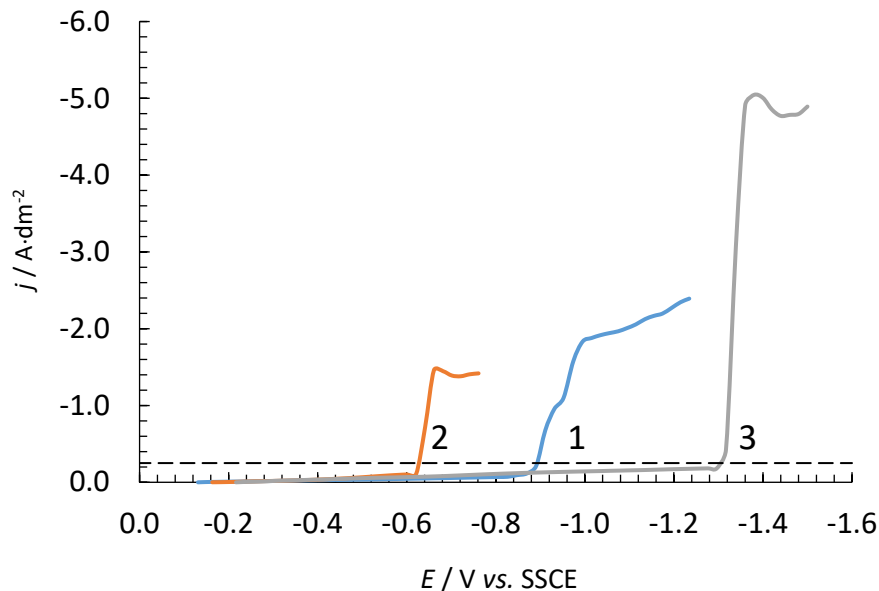


Figure 5. The cathodic potentiodynamic curves (10 mV s^{-1}) obtained in the nickel-plating electrolyte based on DES. Nickel content in the electrolyte is 1.14 M, molar ratio H_2O/Ni : 1: 6; 2: 12; 3: 18. Dashed line shows current density (0.25 A dm^{-2}) where the polarization value was determined

As can be seen from Figure 5, for curve 1 – the limiting current density of the cathode process of electroreduction of nickel in the water-free electrolyte is about 2 A/dm^2 . Compact, gray, velvety nickel deposits were obtained in the current density range of $0.25 - 2.0 \text{ A dm}^{-2}$. The cathodic polarization ΔE , determined for a cathodic current density of 0.25 A dm^{-2} , is about -0.76 V in the electrolyte with molar ratio $H_2O/Ni = 6$.

As the amount of water in the electrolyte increases, the molar ratio $H_2O/Ni = 12$, the ΔE decreases to -0.63 V. The decrease of polarization of the cathodic process is consistent with an increase in the crystal grain size of the nickel deposits on average, from 0.5 to 1.5 μm (Figures 6a, b). In general, the decrease of polarization of the cathodic process can be caused by the change in the structure of the DES-based electrolyte because the addition of water changes the solvation number of nickel ions. As a result, the polarization of the nickel deposition process is lower than that of complex ions based on the studied DES because Ni ions are dissolved in water and not in DES.

A further increase in the amount of water to the molar ratio $H_2O/Ni = 18$ leads to the deeper hydrolysis of the system and the formation of sparingly soluble nickel compounds, which is reflected in the turbidity increase and partial sedimentation of agglomerated species.

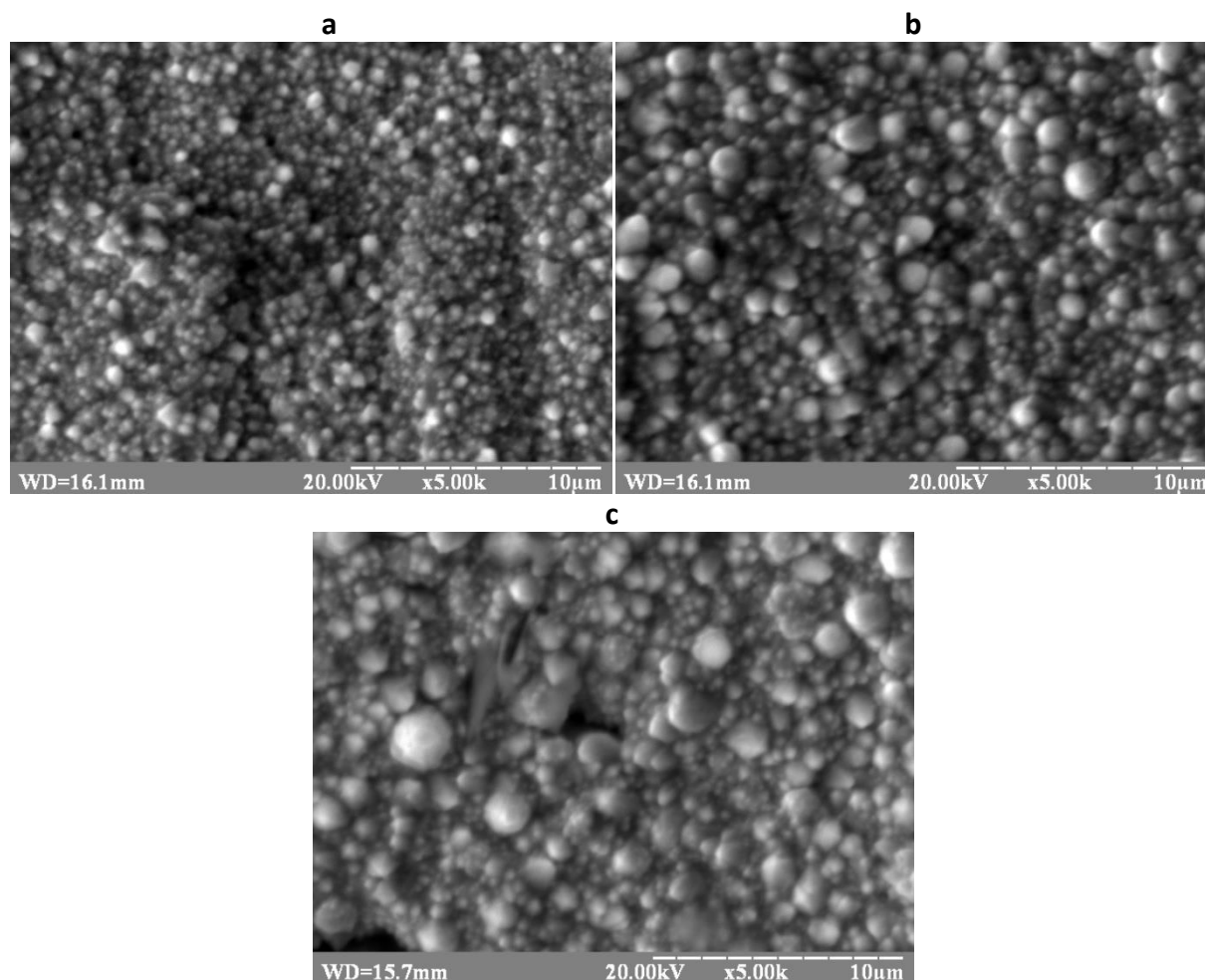


Figure 6. SEM-images of the surface of galvanic nickel deposits with a thickness of 5 μm , obtained in the electrolyte based on DES. Nickel content in the electrolyte 1.14 M, molar ratio H_2O/Ni : 1: 6; 2: 12; 3: 18

The formation of sparingly soluble nickel compounds (Ni salts) leads to partial blockage of the cathode and following an increase in the polarization of the cathodic process, approximately to -1.1 V (Figure 5, curve 3). The increase in the limiting current density can be explained by partial sedimentation and an increase in the metal concentration near the cathode, which was located at a medium level relative to the height of the electrolyte column in the cell. Partial blockage of the cathode leads to a decrease in the homogeneity of the crystal structure and the deterioration of the quality of the nickel deposits (Figure 2, c).

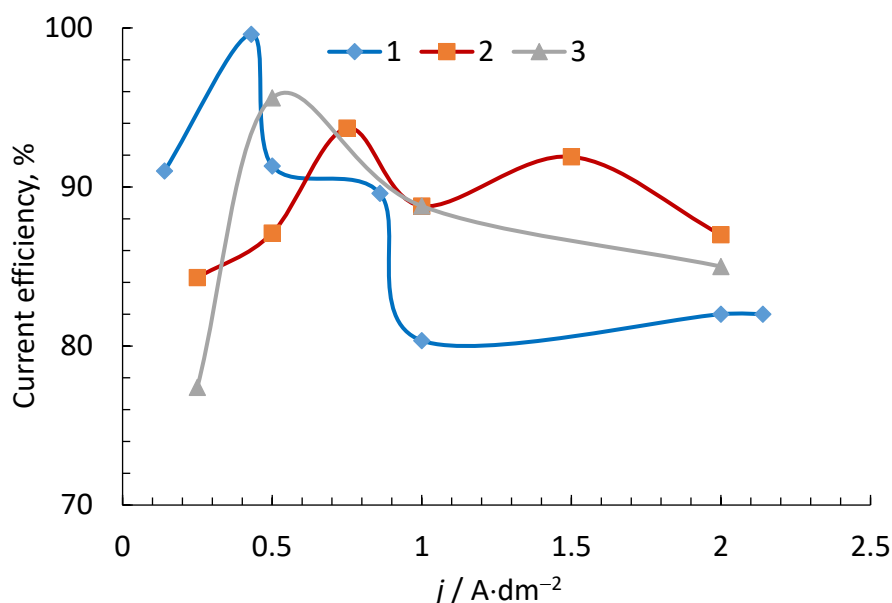
Results of EDX studies of the elemental composition of the sample surfaces with nickel coatings obtained in the studied electrolytes with different amounts of water are given in Table 1.

Table 1. Elemental composition of the surface of nickel coatings with a thickness of 5 μm depending on the amount of water in the electrolyte

H ₂ O/Ni molar ratio	6	12	18
Element	Element content, at. %		
Ni	93.02	94.35	92.13
Fe	5.19	3.28	2.46
O	1.79	2.37	5.41

As can be seen from Table 1, the presence of iron (from steel base) in the coating indicates the porosity of the obtained coatings. As the amount of water in the solution increases, the oxygen content in the surface layers of the coating increases. This may be another confirmation of the fact that the increase in the amount of water in the system increases the amount of sparingly soluble oxygen-containing nickel compounds, which during electrodeposition, are incorporated in the coating.

As shown by the results of determining the current efficiency (Figure 7), the increase in water content in the test solution has little effect on the current efficiency of the nickel deposition process. The current efficiency varies within 80... 97 %, and the maximum values are observed at current densities of 0.5 to 1 $\text{A}\cdot\text{dm}^{-2}$. The main side cathodic process is the molecular hydrogen formation from protons, which is accompanied by intense gas evolution. The lack of a sharp decrease in the current efficiency of nickel deposition from the bath with H₂O/Ni molar ratio = 18 can also be explained by co-deposition with the metal of insoluble nickel compounds.

**Figure 7.** The effect of current density on efficiency for choline chloride - lactic acid DES used for Ni electrodeposition, molar ratio H₂O/Ni 1: 6; 2: 12; 3: 18

An important parameter that determines the throwing power and, as a consequence, the uniformity of current density and coating thickness distribution on the cathode surface is the Wagner number (W). This parameter can be determined by the equation (1) [26]:

$$W = \frac{\sigma}{H} \frac{dE}{dj} = \frac{\sigma}{H} \left(\frac{dj}{dE} \right)^{-1} \quad (1)$$

σ – specific electrical conductivity $S\text{ cm}^{-1}$; H – interelectrode distance, cm; dE/dj – the slope of the polarization curve, $\Omega\text{ cm}^2$. Accordingly, the greater the W , the more uniform and preferred is the secondary distribution of current density. In the case when $W \rightarrow 0$, the uniformity of current and metal distribution decreases, approaches the primary and will be determined by the ratio of the geometric parameters of the galvanic cell. The determined values of electrical conductivity and the calculated dE/dj and W values are given in Table 2. Wagner number was calculated since the interelectrode distance was constant and equal to 2 cm. The slopes were used for the cathodic branches of potentiodynamic curves (Figure 5). Also, according to the data [27], the corresponding electrochemical parameters are given for the Watts electrolyte for comparison.

Table 2. Electrochemical parameters of nickel-plating processes

Parameter	Electrolyte based on the investigated DES with H ₂ O/Ni molar ratio*			Watts electrolyte**[27]
	6	12	18	
$(dE/dj) / \Omega\text{ cm}^2$	6.68	2.96	0.96	2.10
$\sigma / S\text{ cm}^{-1}$	0.009	0.020	0.030	0.700
W	0.030	0.030	0.014	0.740
$\Delta E / V$	-0.76	-0.63	-1.1	-0.4

*temperature 75 °C; **temperature 50 °C.

From Table 2 it can be seen that with the increasing amount of water in the electrolyte, the polarization of the cathode decreases, and the electrical conductivity of the electrolyte increases. The values of the Wagner number for the nickel electrolyte based on the investigated DES are much smaller than for the conventional water-based Watts electrolyte. The values of W in the investigated electrolyte based on DES indicate that the electrodeposition will be dominated by the primary distribution of current density, which is determined by the ratio of the geometric parameters of the cell. Regarding the possible field of application, such an electrolyte can be used in additive technologies of electrochemical 3D printing. In [28], it has been shown that in order to achieve the highest possible accuracy of printing (local electrodeposition of metal) and process control, the electrolyte must have a minimum throwing power, and the current distribution must correspond to the primary one.

Investigation of capillary properties of Ni coatings

Deeper studies of the coating structure showed the presence of a cabbage-like structure with nanosized scaly crystalline groups, the thickness of which is less than 100 nm (Figure 8). In general, the surface of the obtained coatings was gray, coarse-grained and velvety-like (Figure 9a), and the coatings can be easily wetted with water. Similar in appearance and structure tin coatings were already obtained in [29]. The appearance (velvet-like surface) and properties (good wettability of the surface with water) prompted further studies of the capillary properties of the obtained coatings (Figures 9 and 10).

As it was established during the measurement of the height of capillary uplift of ethyl alcohol (Figure 9), on samples obtained from the investigated electrolyte, the capillary rise column reaches 6 mm at a coating thickness of 10 μm and 7-12 mm at a coating thickness of 20 μm . On the matte nickel, electrodeposited from the Watts bath, the alcohol rises by 2 mm, and on the bright nickel, capillary uplift has not been observed.

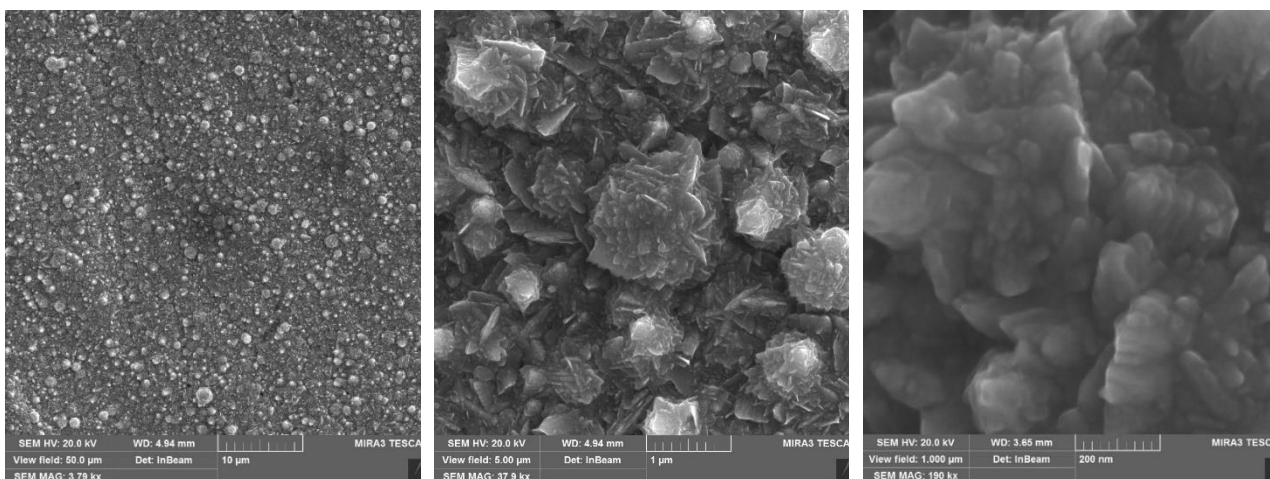


Figure 8. The surface structure (in various magnifications) of the galvanic nickel coating with a thickness of 10 µm, obtained in the electrolyte based on DES. Nickel content in the electrolyte 1.14 M, in the form of $\text{NiCl}_2 \cdot 6\text{H}_2\text{O}$

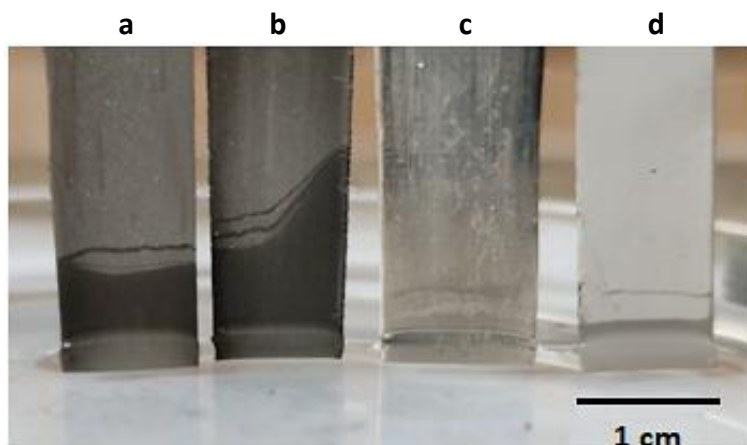


Figure 9. Samples with electrodeposited Ni coatings placed in a container with ethyl alcohol: a, b – electrodeposited from the electrolyte based on DES; c – bright nickel coating; d – matte nickel coating. Coating thickness: a, c, d – 10 µm; b – 20 µm

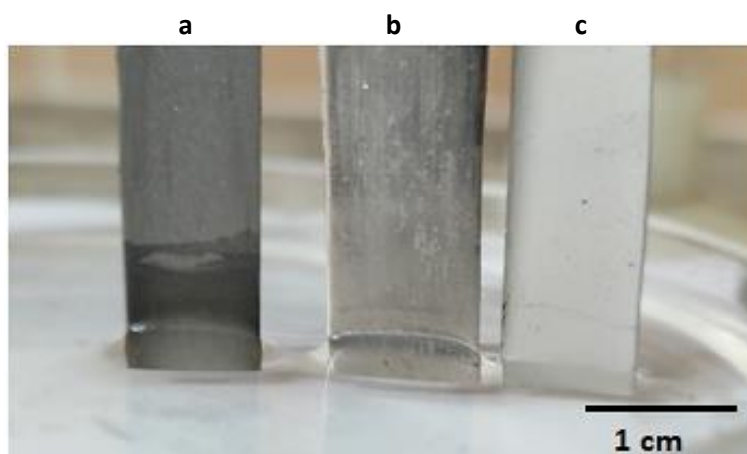


Figure 10. Samples with electrodeposited Ni coatings placed in a container with water: a – electrodeposited from the electrolyte based on DES; b – bright nickel coating; c – matte nickel coating. The thickness of the coatings is 10 µm

On the samples immersed in water (Figure 10), the column of capillary rise of the liquid with a height of 5 mm is observed only on the coatings obtained from the investigated DES-based electrolyte. The thickness of the coating has almost no effect on the height of capillary uplift.

Based on the obtained results, it has been found that electrodeposited nickel coatings from the DES-based electrolyte show the ability of capillary uplift of liquids such as water and ethyl alcohol, compared with conventional matte and bright coatings. This property makes the obtained coating a promising material for heat pipes and heat exchange surface modification [30,31].

The investigation of electrochemical hydrogen evolution reaction

Nickel electrodes are widely used, in particular, in the alkaline electrolysis of water. To reduce energy costs and increase process productivity, electrodes with a highly developed, microstructured, and bulky-porous surface are used [32-34]. The obtained nanostructured surface of nickel coatings that have been electrodeposited from an electrolyte based on DES (Figure 8) may indicate their prospects for use as cathode materials for the electrolysis of water. To investigate the electrochemical activity on the studied electrodes, a linear polarization scan with 10 mV/s scan rate curves was recorded in semilogarithmic coordinates (Figure 11).

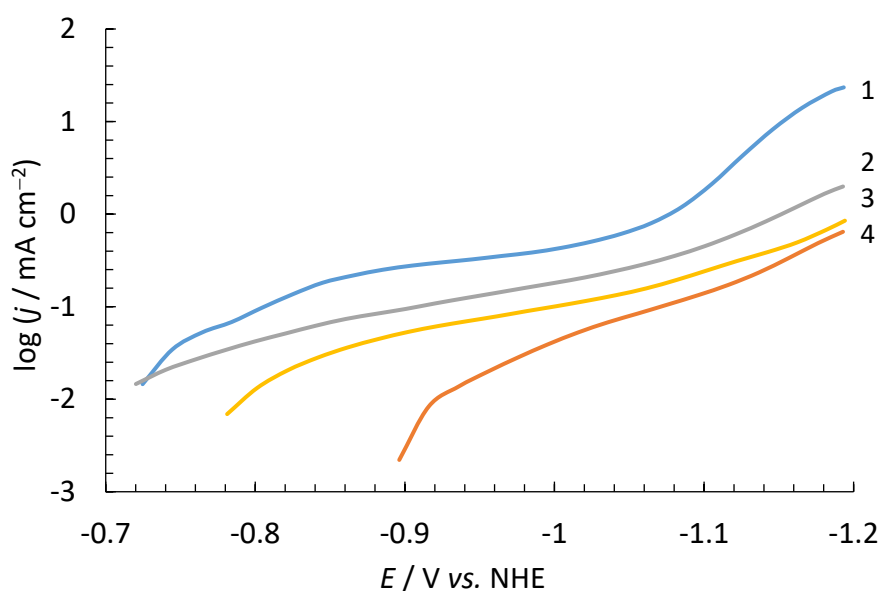


Figure 11. Potentiodynamic polarization curves in 0.1 M KOH and following electrodes:

1 - Pt; 2 - electrodeposited Ni from the electrolyte based on DES;
3 - electrodeposited matte Ni from Watts bath; 4 – electrodeposited bright Ni from Watts bath

From Figure 11, it can be seen that the lowest polarization of hydrogen evolution is observed on platinum, in the second place is nickel electrodeposited from DES-based electrolyte, followed by galvanic matte and bright nickel. Accordingly, at a cathodic current density of 1 mA cm⁻² (log *j* = 0), the potentials of hydrogen evolution are: on platinum at -0.87 V vs. SSCE, on Ni electrodeposited from the electrolyte based on DES at -0.94 V vs. SSCE, on matte and bright nickel about 1 V vs. SSCE. Thus, the obtained data indicate the prospect of using galvanic nickel coatings, electrodeposited from an electrolyte based on a deep eutectic mixture of choline chloride and lactic acid, as cathode materials for electrochemical production of hydrogen.

Conclusions

The deep eutectic mixture of choline chloride and lactic acid with a molar ratio of 1:3 was prepared by the heating method. The FT-IR analysis proved the formation of the combined bonding of choline chloride and lactic acid molecules and the ¹H NMR analysis proved the molar ratio of the

choline chloride – lactic acid to be 1:3. The electrochemical stability window was found to be 1.33 V for pure DES and reduces to 1.3 V when water was added in the amount of 25 vol.%.

During the investigation of the process of electrodeposition of nickel coatings from the electrolyte based on a deep eutectic mixture of choline chloride and lactic acid, the following have been established. The surface of the electrodeposited coatings is light gray, like velvet. Galvanic deposits of nickel are quite coarse-grained with a grain size of 0.5 to 2 μm . The surface of the crystal grains is highly developed and contains scaly crystals with a characteristic size of less than 100 nm. Galvanic coatings, which were electrodeposited from the investigated electrolyte, show quite pronounced capillary properties in relation to water and ethyl alcohol.

The highly developed surface structure of the obtained coatings makes them promising for use as an electrode material for hydrogen evolution reaction. The height of the capillary rise column on investigated coatings is 4 to 6 times higher than that on conventional matte and bright coatings obtained by Watts bath. As the water concentration in the electrolyte increases ($\text{H}_2\text{O}/\text{Ni}$ molar ratio increases from 6 to 8), the electrical conductivity of the system increases from 0.009 to 0.03 S/cm. However, the increase in the amount of water contributes to the deterioration and electrodeposition of more coarse-grained and less-ordered structures of nickel deposits. It has been established that in the range of current densities of 0.25 to 2 A dm^{-2} the current efficiency of nickel deposition process varies within 80 to 97 %. Increasing the amount of water in the electrolyte does not significantly affect the current efficiency.

Based on polarization measurements and electrical conductivity measurements, the values of the Wagner number are determined, which vary within 0.014 to 0.03. The obtained values indicate the predominance of the primary current density distribution during the electrodeposition of nickel from the electrolyte based on a deep eutectic mixture of choline chloride and lactic acid. This makes promising the use of the corresponding electrolyte in additive technologies, in particular, systems of electrochemical 3D-printing.

The investigation of the hydrogen electrochemical reduction process showed that the polarization of this process on electrodeposited nickel coatings from the DES-based electrolyte is 60 mV lower than that on matte and bright nickel coatings.

Acknowledgments: *The work was supported by the Ministry of science and education of Ukraine, grant number 2403, 2022.*

References

- [1] B. B. Hansen, S. Spittle, B. Chen, D. Poe, Y. Zhang, J. M. Klein, A. Horton, L. Adhikari, T. Zelovich, B. W. Doherty, B. Gurkan, E. J. Maginn, A. Ragauskas, M. Dadmun, T.A. Zawodzinski, G. A. Baker, M. E. Tuckerman, R. F. Savinell, J. R. Sangoro, Deep eutectic solvents: A review of fundamentals and applications, *Chemical Reviews* **121** (2021) 1232-1285. <https://doi.org/10.1021/acs.chemrev.0c00385>
- [2] G. Di Carmine, A. P. Abbott, C. D'Agostino, Deep eutectic solvents: alternative reaction media for organic oxidation reactions, *Reaction Chemistry & Engineering* **6** (2021) 582-598. <https://doi.org/10.1039/D0RE00458H>
- [3] A. P. Abbott, K. J. Edler, A. J. Page, Deep eutectic solvents—The vital link between ionic liquids and ionic solutions, *Journal of Chemical Physics* **155** (2021) 150401. <https://doi.org/10.1063/5.0072268>
- [4] L. Lomba, M.P. Ribate, E. Sangüesa, J. Concha, M. P. Garralaga, D. Errazquin, C. B. García, B. Giner, Deep eutectic solvents: Are they safe?, *Applied Science* **11** (2021) 10061. <https://doi.org/10.3390/app112110061>

- [5] T. El Achkar, H. Greige-Gerges, S. Fourmentin, Basics and properties of deep eutectic solvents: a review, *Environmental Chemistry Letters* **19** (2021) 3397-3408. <https://doi.org/10.1007/s10311-021-01225-8>
- [6] K. M. Kuehn, C.M. Massmann, N.R. Sovell, Choline chloride eutectics: Low temperature applications, *Journal of Undergraduate Research* **15** (2017) 5. <https://openprairie.sdstate.edu/jur/vol15/iss1/5>
- [7] R. Bernasconi, G. Panzeri, A. Accogli, F. Liberale, L. Nobili, L. Magagnin, *Progress and developments in ionic liquids*, IntechOpen, London, United Kingdom, 2017, 235-254. <https://doi.org/10.5772/64935>
- [8] K. L. Fow, M. Ganapathi, I. Stassen, K. Binnemans, J. Fransaer, D.E. De Vos, Catalytically active gauze-supported skeletal nickel prepared from Ni–Zn alloys electrodeposited from an acetamide–dimethyl sulfone eutectic mixture, *Catalysis Today* **246** (2015) 191-197. <https://doi.org/10.1016/j.cattod.2014.10.028>
- [9] A.P. Abbott, A. Ballantyne, R.C. Harris, J.A. Juma, K.S. Ryder, Bright metal coatings from sustainable electrolytes: The effect of molecular additives on electrodeposition of nickel from a deep eutectic solvent, *Physical Chemistry Chemical Physics* **19** (2017) 3219-3231. <https://doi.org/10.1039/c6cp08720e>
- [10] L.H. Xua, D. Wu, M. Zhong, G.B. Wang, X.Y. Chen, Z.J. Zhang, The construction of a new deep eutectic solvents system based on choline chloride and butanediol: The influence of the hydroxyl position of butanediol on the structure of deep eutectic solvent and supercapacitor performance, *Journal of Power Sources* **490** (2021) 229365. <https://doi.org/10.1016/j.jpowsour.2020.229365>
- [11] M.K. Tran, M.-T.F. Rodrigues, K. Kato, G. Babu, P.M. Ajayan, Deep eutectic solvents for cathode recycling of Li-ion batteries, *Nature Energy* **4** (2019) 339-345. <https://doi.org/10.1038/s41560-019-0368-4>
- [12] M. E. Di Pietro, A. Melea, Deep eutectics and analogues as electrolytes in batteries, *Journal of Molecular Liquids* **338** (2021) 116597. <https://doi.org/10.1016/j.molliq.2021.116597>
- [13] J. Winiarski, A. Niciejewska, J. Ryl, K. Darowicki, S. Baśladyńska, K. Winiarska, B. Szczygieł, Ni/cerium molybdenum oxide hydrate microflakes composite coatings electrodeposited from choline chloride: Ethylene glycol deep eutectic solvent, *Materials* **13** (2020) 924-941. <https://doi.org/10.3390/ma13040924>
- [14] A.P. Abbotta, A. Ballantyne, R.C. Harris, J.A. Jumma, K.S. Ryder, G. Forrest, Comparative study of nickel electrodeposition using deep eutectic solvents and aqueous solutions, *Electrochimica Acta* **176** (2015) 718-726. <https://doi.org/10.1016/j.electacta.2015.07.051>
- [15] S.P. Rosoiu, A.G. Pantazi, A. Petica, A. Cojocar, S. Costovici, C. Zanella, T. Visan, L. Anicai, M. Enachescu, Comparative study of Ni-Sn alloys electrodeposited from choline chloride-based ionic liquids in direct and pulsed current, *Coatings* **9** (2019) 801-815. <https://doi.org/10.3390/coatings9120801>
- [16] S. Costovici, A.-C. Manea, T. Visan, L. Anicai, Investigation of Ni-Mo and Co-Mo alloys electrodeposition involving choline chloride based ionic liquids, *Electrochimica Acta* **207** (2016) 97-111. <https://doi.org/10.1016/j.electacta.2016.04.173>
- [17] E. Gutierrez, J. A. Rodriguez, J. Cruz-Borbolla, Y. Castrillejo, E. Barrado, Effect of deep eutectic solvent composition on the corrosion behavior of electrodeposited cadmium coatings on carbon steel, *International Journal of Electrochemical Science* **13** (2018) 11016-11023. <https://doi.org/10.20964/2018.11.83>
- [18] P. Cojocar, L. Magagnin, E. Gomez, E. Vallés, Using deep eutectic solvents to electrodeposit CoSm films and nanowires, *Materials Letters* **65** (2011) 3597-3600. <https://doi.org/10.1016/j.matlet.2011.08.003>

- [19] C. Fanali, V. Gallo, S. D. Posta, L. Dugo, L. Mazzeo, M. Cocchi, V. Piemonte, L. De Gara, Choline chloride–lactic acid-based NADES as an extraction medium in a response surface methodology-optimized method for the extraction of phenolic compounds from hazelnut skin, *Molecules* **26** (2021) 2652. <https://doi.org/10.3390/molecules26092652>
- [20] Q. Bao, L. Zhao, H. Jing, A. Mao, Electrodeposition of zinc from low transition temperature mixture formed by choline chloride + lactic acid, *Materials Today Communications* **14** (2018) 249-253. <https://doi.org/10.1016/j.mtcomm.2018.01.015>
- [21] A. Skulcova, A. Russ, M. Jablonsky, J. Sima, The pH behavior of seventeen deep eutectic solvents, *Biological Research* **13** (2018) 5042-5051. <https://doi.org/10.15376/biores.13.3.5042-5051>
- [22] V.I. Vorobyova, O.V. Linyucheva, O.E. Chygyrynets, M.I. Skiba, G.S. Vasyliiev, Comprehensive physicochemical evaluation of deep eutectic solvents: quantum-chemical calculations and electrochemical stability, *Molecular Crystals and Liquid Crystals*, May 2022. <https://doi.org/10.1080/15421406.2022.2073037>
- [23] G. Vasyliiev, L. Khrokalo, K. Hladun, M. Skiba, V. Vorobyova, Valorization of tomato pomace: extraction of value-added components by deep eutectic solvents and their application in the formulation of cosmetic emulsions, *Biomass Conversion and Biorefinery* **12** (2022) 95-111. <https://doi.org/10.1007/s13399-022-02337-z>
- [24] R. Alcalde, A. Gutiérrez Vega, M. Atilhan, S. Aparicio, An experimental and theoretical investigation of the physicochemical properties on choline chloride – Lactic acid based natural deep eutectic solvent (NADES), *Journal of Molecular Liquids* **290** (2019) 110916. <https://doi.org/10.1016/j.molliq.2019.110916>
- [25] F.I. Danilov, V.S. Protsenko, A.A. Kityk, D.A. Shaiderov, E.A. Vasil'eva, U.P. Kumar, C.J. Kennady, Electrodeposition of nanocrystalline nickel coatings from a deep eutectic solvent with water addition, *Protection of Metals and Physical Chemistry of Surfaces* **53** (2017) 1131-1138. <https://doi.org/10.1134/S2070205118010203>
- [26] J.O. Dukovic, *Current Distribution and Shape Change in Electrodeposition of Thin Films for Microelectronic Fabrication*, Chap.3 in: *Advances in Electrochemical Science and Engineering*, Vol. 3, H. Gerischer, C.W. Tobias, (Eds.), Wiley-VCH, Weinheim, 1993, 117-161. <https://doi.org/10.1002/9783527616770.ch3>
- [27] D.Yu. Ushchapovskiy, O.V. Linyucheva, R.M. Redko, A.I. Kushmyruk, A.S. Zabaluev, *Simulation approach in the development of polyfunctional electrode materials*, in: *Promising Materials and Processes in Applied Electrochemistry*, monograph, Kyiv National University of Technologies and Design, Kyiv, Ukraine, 2020, 70-79. https://er.knutd.edu.ua/bitstream/123456789/17001/1/Promising_2020_P070-079.pdf
- [28] G. Vasyliiev, V. Vorobyova, D. Ushchapovskiy, O. Linyucheva, Local electrochemical deposition of copper from sulfate solution, *Journal of Electrochemical Science and Engineering* **12** (2022) 557-563. <https://doi.org/https://doi.org/10.5599/jese.1352>
- [29] D.Yu. Ushchapovskiy, O.V. Linyucheva, T.I. Motronyuk, H.Yu. Podvashetskiy, Electrodeposited nanostructured polyfunctional tin-based electrocatalyst, *Journal of Chemistry and Technologies* **29** (2021) 363-369. <https://doi.org/10.15421/jchemtech.v29i3.236134>
- [30] J.K. Abdali, A.A. Alwan, R.H. Hameed, Heat pipe and applications-recent advances and review, *Test Engineering and Management* **83** (2020) 13182-13198. <https://www.researchgate.net/publication/344442623>
- [31] A. M. Gheitaghy, H. Saffari, M. Mohebbi, Investigation pool boiling heat transfer in U-shaped mesochannel with electrodeposited porous coating, *Experimental Thermal and Fluid Science*, **76** (2016) 87-97. <https://doi.org/10.1016/j.expthermflusci.2016.03.011>

- [32] R. Ding, S. Cui, J. Lin, Z. Sun, P. Du, C. Chen, Improving the water splitting performance of nickel electrodes by optimizing their pore structure using a phase inversion method, *Catalysis Science & Technology* **7** (2017) 3056-3064. <https://doi.org/10.1039/C7CY00519A>
- [33] H. Yin, L. Jiang, P. Liu, M. Al-Mamun, Y. Wang, Y.L. Zhong, H. Yang, D. Wang, Z. Tang, H. Zhao, Remarkably enhanced water splitting activity of nickel foam due to simple immersion in a ferric nitrate solution, *Nano Research* **11** (2018) 3959-3971. <https://doi.org/10.1007/s12274-017-1886-7>
- [34] X. Gao, Y. Chen, T. Sun, J. Huang, W. Zhang, Q. Wang, R. Cao, Karst landform-featured monolithic electrode for water electrolysis in neutral media, *Energy & Environmental Science* **13** (2020) 174-182. <https://doi.org/10.1039/C9EE02380A>

